



AFRL-RX-WP-TP-2012-0375

**ANALYSIS OF DEFORMATION SUBSTRUCTURES IN A
NOTCHED LCF SAMPLE UNDER DWELL CONDITION IN
A Ni-BASED SUPERALLOY (PREPRINT)**

**G.B. Viswanathan, S. Jha, J. Tiley and Christopher Woodward
Metals Branch
Structural Materials Division**

**Ken Bain
GE Aviation**

**Dan Huber, S. Sam, and H.L. Fraser
Ohio State University**

**August 2012
Interim**

Approved for public release; distribution unlimited.

See additional restrictions described on inside pages

STINFO COPY

**AIR FORCE RESEARCH LABORATORY
MATERIALS AND MANUFACTURING DIRECTORATE
WRIGHT-PATTERSON AIR FORCE BASE, OH 45433-7750
AIR FORCE MATERIEL COMMAND
UNITED STATES AIR FORCE**

REPORT DOCUMENTATION PAGE				Form Approved OMB No. 0704-0188	
The public reporting burden for this collection of information is estimated to average 1 hour per response, including the time for reviewing instructions, searching existing data sources, gathering and maintaining the data needed, and completing and reviewing the collection of information. Send comments regarding this burden estimate or any other aspect of this collection of information, including suggestions for reducing this burden, to Department of Defense, Washington Headquarters Services, Directorate for Information Operations and Reports (0704-0188), 1215 Jefferson Davis Highway, Suite 1204, Arlington, VA 22202-4302. Respondents should be aware that notwithstanding any other provision of law, no person shall be subject to any penalty for failing to comply with a collection of information if it does not display a currently valid OMB control number. PLEASE DO NOT RETURN YOUR FORM TO THE ABOVE ADDRESS.					
1. REPORT DATE (DD-MM-YY) August 2012		2. REPORT TYPE Technical Paper		3. DATES COVERED (From - To) 1 July 2012 – 1 August 2012	
4. TITLE AND SUBTITLE ANALYSIS OF DEFORMATION SUBSTRUCTURES IN A NOTCHED LCF SAMPLE UNDER DWELL CONDITION IN A Ni-BASED SUPERALLOY (PREPRINT)				5a. CONTRACT NUMBER FA8650-08-C-5226	
				5b. GRANT NUMBER	
				5c. PROGRAM ELEMENT NUMBER 62102F	
6. AUTHOR(S) G.B. Viswanathan, S. Jha, J. Tiley and Christopher Woodward (AFRL/RXCM) Ken Bain (GE Aviation) Dan Huber, S. Sam, and H.L. Fraser (Ohio State University)				5d. PROJECT NUMBER 4347	
				5e. TASK NUMBER	
				5f. WORK UNIT NUMBER LM114100	
7. PERFORMING ORGANIZATION NAME(S) AND ADDRESS(ES) University of North Texas Corner of Avenue C Chestnut Denton, TX 76203				8. PERFORMING ORGANIZATION REPORT NUMBER	
9. SPONSORING/MONITORING AGENCY NAME(S) AND ADDRESS(ES) Air Force Research Laboratory Materials and Manufacturing Directorate Wright-Patterson Air Force Base, OH 45433-7750 Air Force Materiel Command United States Air Force				10. SPONSORING/MONITORING AGENCY ACRONYM(S) AFRL/RXCM	
				11. SPONSORING/MONITORING AGENCY REPORT NUMBER(S) AFRL-RX-WP-TP-2012-0375	
12. DISTRIBUTION/AVAILABILITY STATEMENT Approved for public release; distribution unlimited. Preprint to be submitted to Superalloys 2012.					
13. SUPPLEMENTARY NOTES The U.S. Government is joint author of this work and has the right to use, modify, reproduce, release, perform, display, or disclose the work. PA Case Number and clearance date: 88ABW-2012-2969, 21 May 2012. This document contains color.					
14. ABSTRACT Detailed transmission electron microscopy (TEM) studies were conducted on LCF René 104 alloy samples tested under dwell conditions to analyze the deformation substructures. Specifically, the focus was to investigate the effect of crack length, in other words, stress intensity factor range ΔK , on the deformation substructures. Thin foils were prepared by focused ion beam method (FIB) from two specific grains along the crack path at varying distances representing varying K values. The TEM analysis indicated that the character of deformation substructures significantly differed in these two grains. It is therefore speculated that local stress conditions and the grain orientations played a key role in the damage accumulation and subsequent substructure evolution. The regions below the fracture surface also investigated were. Detailed scanning electron microscopy (SEM) investigations of the grains immediately below the fracture surface revealed extensive microstructure degradation and and potential hot spots for crack nucleation.					
15. SUBJECT TERMS transmission electron microscopy, dislocations, deformation, low cycle fatigue, dwell-fatigue, superalloy					
16. SECURITY CLASSIFICATION OF:			17. LIMITATION OF ABSTRACT: SAR	NUMBER OF PAGES 10	19a. NAME OF RESPONSIBLE PERSON (Monitor) Jaimie Tiley 19b. TELEPHONE NUMBER (Include Area Code) N/A
a. REPORT Unclassified	b. ABSTRACT Unclassified	c. THIS PAGE Unclassified			

ANALYSIS OF DEFORMATION SUBSTRUCTURES IN A NOTCHED LCF SAMPLE UNDER DWELL CONDITION IN A Ni-BASED SUPERALLOY

G.B.Viswanathan¹, Ken Bain², Dan Huber³, S. Jha¹, S. Sam³, J. Tiley¹, Christopher Woodward¹ and H.L. Fraser³

¹ Air Force Research Laboratory, Wright-Patterson AFB, OH 45433

² GE Aviation, Cincinnati, OH 45215

³ Department of Materials Science and Engineering, The Ohio State University, OH 43210

Keywords: transmission electron microscopy, dislocations, deformation, low cycle fatigue, dwell-fatigue, superalloy

Abstract:

Detailed transmission electron microscopy (TEM) studies were conducted on LCF René 104 alloy samples tested under dwell conditions to analyze the deformation substructures. Specifically, the focus was to investigate the effect of crack length, in other words, stress intensity factor range ΔK , on the deformation substructures. Thin foils were prepared by focused ion beam method (FIB) from two specific grains along the crack path at varying distances representing varying K values. The TEM analysis indicated that the character of deformation substructures significantly differed in these two grains. It is therefore speculated that local stress conditions and the grain orientations played a key role in the damage accumulation and subsequent substructure evolution. The regions below the fracture surface also investigated were. Detailed scanning electron microscopy (SEM) investigations of the grains immediately below the fracture surface revealed extensive microstructure degradation and potential hot spots for crack nucleation.

Introduction:

The ability to resist crack growth under dwell-fatigue is a complex phenomenon in polycrystalline Ni-based superalloys used for turbine engine disk applications. Whether or not the fatigue process is controlled in a time independent manner (typically seen at low temperatures and higher cyclic frequency > 1 Hz or in time-dependent manner (seen at high temperatures, low cyclic frequency < 1 Hz or longer hold time between cycles), the fatigue crack growth rate (FCGR) is significantly higher in samples tested in an air environment compared to vacuum [1-3]. As a result, the debit in fatigue life has been attributed to the diffusion of oxygen into slip bands causing further slip-band-hardening ahead of the advancing crack [4]. In the latter case the debit is attributed to diffusion of oxygen to the grain boundaries making them fail prematurely. Accordingly, numerous studies, listed in ref. 3 have reported the failure mode switching from transgranular to mixed-mode to entirely intergranular fracture. These failure modes can be significantly influenced further by factors such as temperature, hold time duration. More importantly, the microstructure has a major influence on FCGR. While the effect of microstructural features such as grain size [3] and grain boundary phases on low cycle fatigue are largely known [3], the understanding of the deformation substructure evolution ahead of the crack in the presence of γ and γ' phases is still developing. This understanding is extremely important in designing the optimum heat-treatment for these alloys to balance the high temperature hold time crack growth resistance against creep properties.

Deformation by planar slip has been the central outcome of deformation studies in almost all of Ni-based superalloys evaluated under diverse loading conditions both at room temperature and at intermediate temperatures up to 700°C. Reported planar deformation processes include shearing of both γ and γ' by (i) strongly paired $\frac{1}{2}[110]$ unit dislocations, (ii) decorrelated $1/6\langle 112 \rangle$ type Shockley partials causing intrinsic and extrinsic stacking faults [5,6] and micro-twinning [6,7]. These diverse deformation processes operate either individually or in combination depending on the temperature and the loading condition [6,7]. While numerous previous studies have focused on elucidating the deformation mechanism both during creep and during fatigue, only a handful of studies have paid attention to the deformation substructures during dwell-fatigue [8], which by definition exhibits creep alike condition between successive fatigue cycles. In this study, the primary focus is to study deformation substructures in notched samples of René 104, a Ni-base superalloy tested under low cycle fatigue condition with hold-time dwell. Specifically, this study concentrates on the effect of varying ΔK , the stress intensity range, on the development of substructures. This is accomplished by primarily investigating deformation substructures of different grains at varying distances along the crack path for their deformation substructures.

Experimental Details:

René 104, the Ni-based superalloy used in this study is a powder processed polycrystalline alloy. The alloy was supersolvus heat-treated and had a coarse grain microstructure (grain size 15-30 μm). The specimens were mechanically polished using standard metallographic processes and finished with 0.05 colloidal silica in a vibratory polishing unit. SEM techniques were used to characterize the microstructure of the specimens. Samples were etched with a γ' etchant (2 ml HF, 20 ml HNO₃ and 50 ml lactic acid), and imaged in the SEM with a back scattered electron (BSE) detector in "ultra-high resolution" (UHR) mode. Additional information on the imaging techniques are detailed elsewhere [9].

The dwell fatigue tests were conducted at GE Aviation, Evendale at two different temperatures. The samples were tested at (i) 704°C(1300°F), R=0.05, $K_f=1.77$, Peak Load 848 MPa (123 ksi) The sample was tested at this temperature with a 90 second dwell time between the cycles.

The fracture morphology of the fatigue samples was investigated in the SEM. Metallographic samples were prepared normal to the fracture surface to investigate the region beneath for fatigue damage. Site-specific thin foils were extracted by focused ion beam method (FIB) at various distances from the notched edge of

the samples along the crack path, both from the fracture surface and from grains beneath the fracture surface. The foils were used to examine the damage mechanisms as a function of crack using an FEI, Tecnai-200 kV transmission electron microscope (TEM).

Results

Figure 1a shows the typical starting microstructures of the alloy tested in this study. The super-solvus heat treatment resulted in

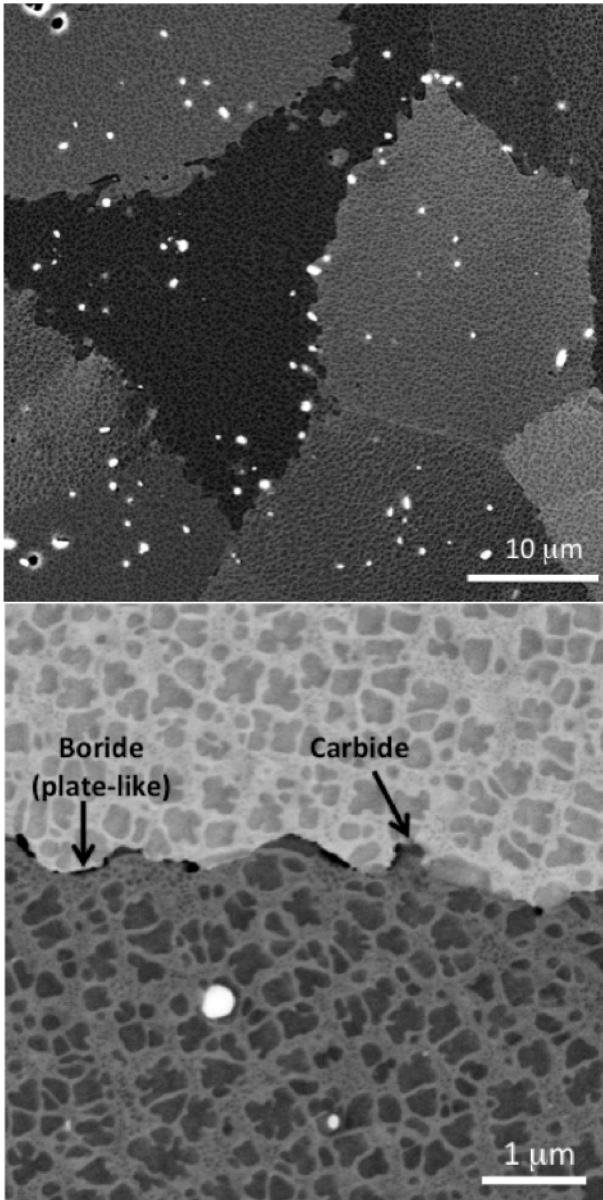


Figure 1. Back scattered electron (BSE) images showing (a) typical microstructure of the alloy, bright colored carbide particles can be seen distributed (b) higher magnification image of a typical grain boundary decorated with carbide and boride particles. Bi-modal distribution of γ' precipitates can be seen within the grains.

coarse grain structure (15-30 μm) with secondary and tertiary γ' precipitates in the grain interior, and carbides and borides at the grain boundaries. Blocky carbide particles can also be seen in the

grain interior (Figure 1b). The borides at the boundaries are thin,

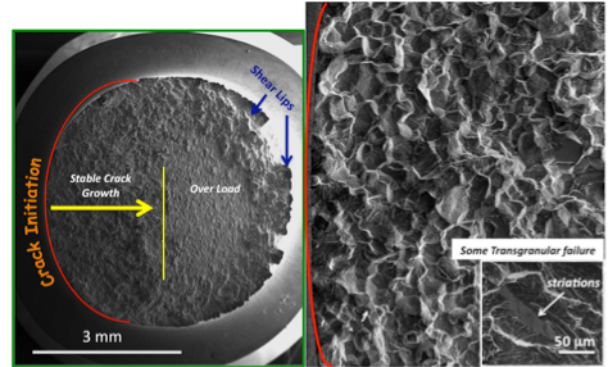


Figure 2 Secondary electron image showing: (a) the entire fracture surface of the dwell fatigue sample (b) the mixed-mode nature of failure near the notched edge of the sample.

elongated and plate-like. The SEM image shown in Figure 2 delineates different regions of the fracture surface. The fatigue cracks seem to have initiated at multiple locations on the surface of the notched samples. The rest of the fracture surface can be divided into two regions, (i) the stable crack growth region where the fracture mode is mostly mixed-mode where significant number of grains can be seen fractured in trans-granular fashion and (ii) the unstable crack growth region where the fracture is entirely trans-granular. Secondary cracks can be seen near these grains well.

The information that can be obtained from the SEM image of the fracture was rather limited. On the other hand the investigation of

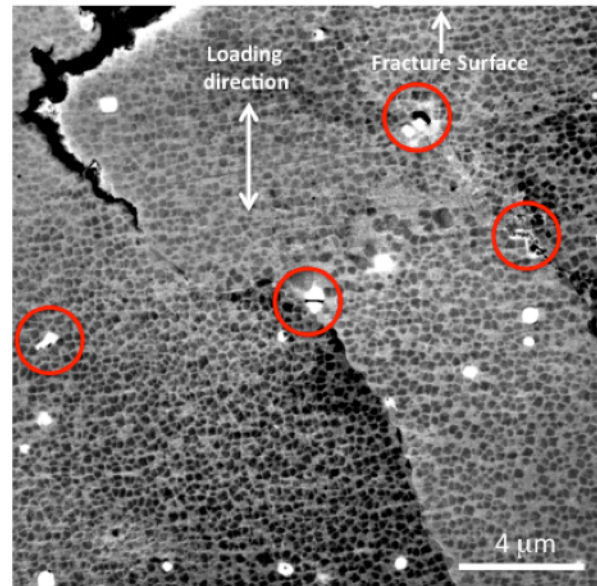


Figure 3 Back scattered electron (BSE) image showing the crack propagation through grain boundary. Circled regions are the cracked carbide particles.

the region immediately beneath the fracture surface was very informative. Secondary intergranular cracking evident in Figure 3. The mottled contrast from the grain interior arises from the severe deformation the adjoining grains undergo associated with the crack advance along the grain boundaries. Cracks can be seen nucleating along the carbide/matrix interface. Interestingly, carbide particles themselves appear cracked in the grain interior.

This indicates the severity of the deformation of the grains along the fracture path. Nucleation of cracks at grain triple junctions is

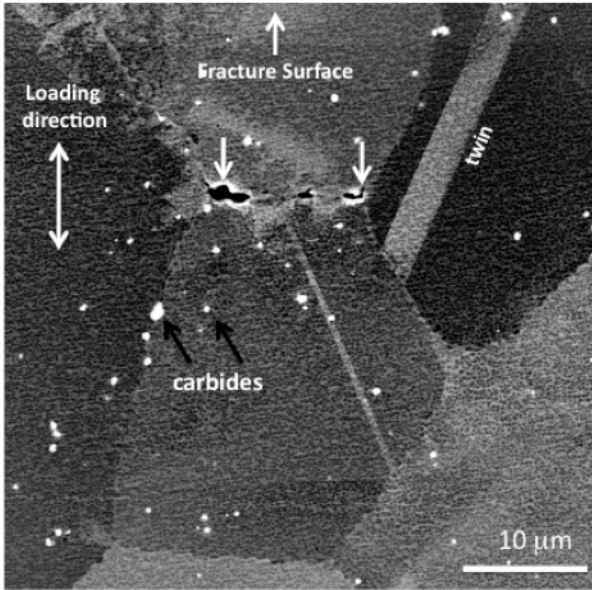


Figure 4. Back scattered electron (BSE) image showing intergranular crack nucleation at the triple grain junctions

also seen frequently occurring as shown in Figure 4. Another interesting observation is the change in the microstructure in the

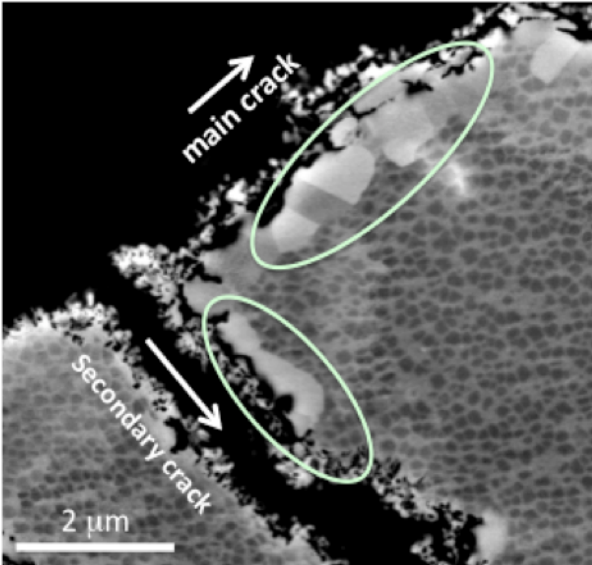


Figure 5. Back scattered electron (BSE) image showing recrystallization and the loss of γ' immediately beneath the fracture surface.

grain immediately beneath the fracture surface that was exposed to high temperature during the fatigue. The exposed regions of the grain, as seen in Figure 5 show evidence of recrystallization of new smaller grains. In those regions, significant portion of γ' precipitates seem to have dissolved.

Figure 6 shows a FIB extraction of a slice, which was taken approx. 1100 microns from the surface of the notch. This equates

to a ΔK of XXX. The TEM investigation of the deformation substructures from thin foils extracted from two different locations on the fracture surface are shown in Figures 7 through 9.

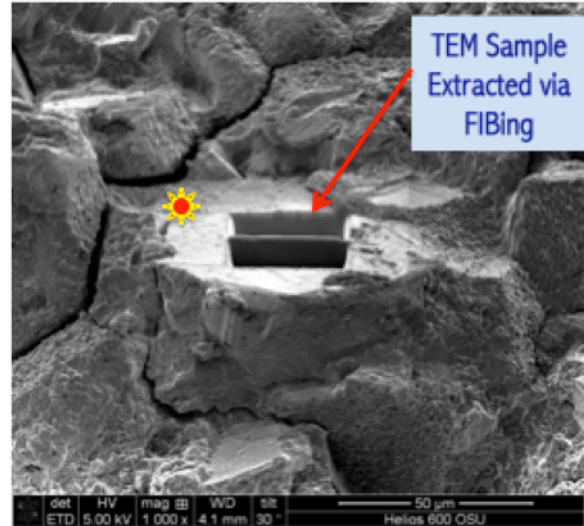


Figure 6 Secondary electron (SE) image showing TEM thin foil extraction from the fracture surface.

Grains from regions of high and low ΔK were approximately 1100 and 300 microns from the crack initiation site respectively. Assuming these distances equal the crack lengths at these distances and using the K solution expression given below, these grains have ΔK values of approximately 45 and 20 $\text{MPa}\cdot\text{m}^{1/2}$ respectively.

$$\Delta K = F\left(\frac{a}{D}\right)\Delta\sigma\sqrt{\pi a}$$

where $\Delta\sigma$ is the applied stress range, a is the crack depth and D is net diameter of the specimen on the notched plane.

In general, Figures 7 through 9 show that the dislocation density is very high in samples extracted from both locations consistent with the fact that these grains have been severely deformed due to crack propagations through them. There are both commonalities and differences in the nature of the substructures between the grains from regions of low and high low and high ΔK . In both grains the defect density is extremely high in the γ matrix compared to the γ' precipitates. Both grains have planar and non-planar deformation substructures although the relative amounts of these are difficult to estimate at the present time. There are no incidences of micro-twin formation in both of these grains, which have been reported to be the operating mechanism during creep at these temperatures [7]. The absence of twinning is also consistent with the fact that more non-planar deformation modes begin operating under dwell-fatigue conditions. The occurrence of planar and non-planar deformation is not only limited to γ matrix. For example, Figure 8 shows the shearing of γ' precipitates by cross-slip. Detailed tilting analysis in the TEM has shown (Figure 8) segments of strongly paired $b=1/2[110]$ dislocations (marked by arrows) on the $[001]$ cube planes. Cube cross slip is a well-known phenomena known to occur at high temperatures.

On the other hand, there are significant differences between the deformation substructures between the samples. The deformation

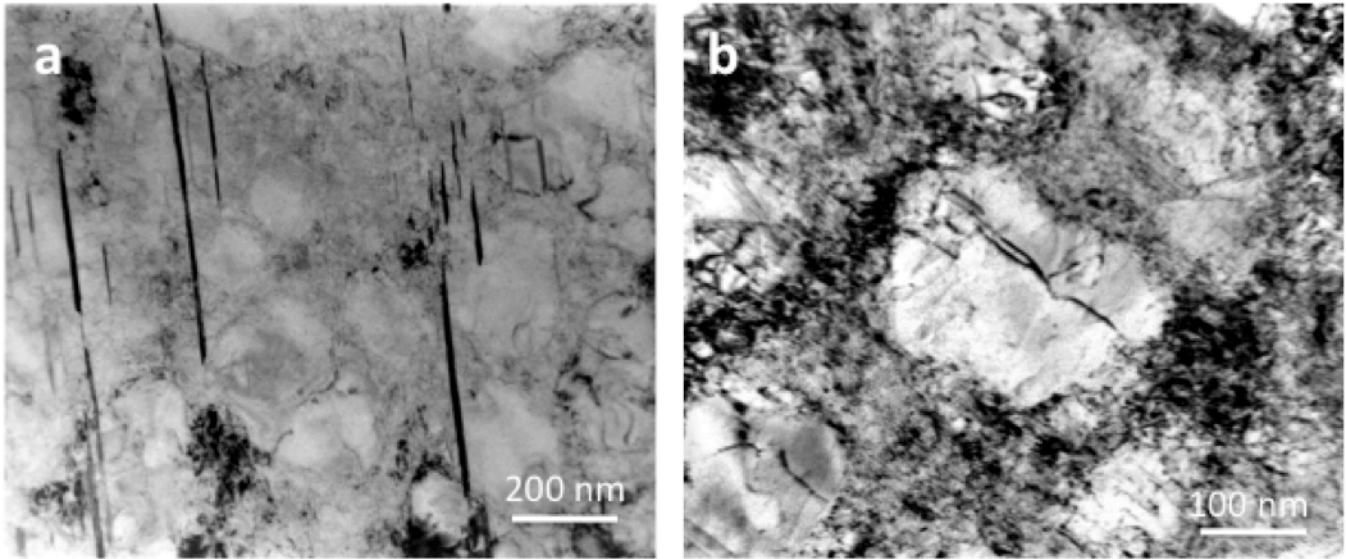


Figure 7 Bright field transmission electron microscopy (TEM) images showing (a) limited extended faulting and (b) extensive dislocation activity in both γ matrix and γ' precipitates; in grain with low Δk grain.

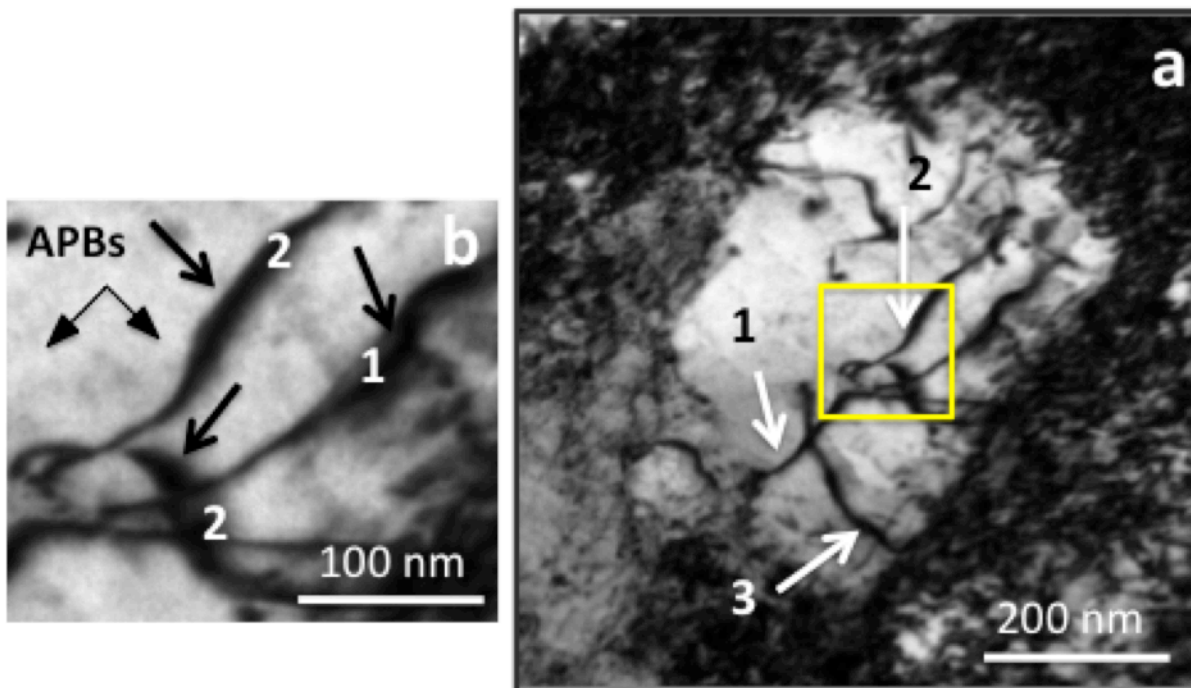


Figure 8. Bright field TEM images from grain with low Δk showing (a) $\frac{1}{2}[110]$ superpartials (marked 1 through 3) shearing the γ' precipitate. (b) the perpendicular segments of the superpartial # 2 have the cross slipped onto cube planes.

substructures in the grain from the low delta K regime consists of $\frac{1}{2}[110]$ unit dislocations mostly in the gamma matrix. In addition cross slipping of dislocations on to cube planes were seen within the γ' precipitates in the same grain. Conversely, the grain in the regime of high delta K contains a significant density of stacking faults (Figure 9) in the gamma matrix beside the dislocations. Analysis has shown that these are intrinsic stacking faults bounded by Shockley partial dislocations. De-correlated partial dislocations have been known to form during high temperature

creep. Incidences of planar shearing of γ' pre cipitates by strongly paired $b=\frac{1}{2}[110]$ dislocations are more frequently seen in this sample compared to that of sample 1 where much more incidences of cube cross-slip based non-planar shearing were observed. The weak beam dark field image in Figure 8 shows strongly paired $\frac{1}{2}[110]$ (111) dislocations within the γ' precipitate. The dislocation debris in both samples is an important substructures feature not frequently seen in other high temperature deformation modes.

Discussion:

The advantage afforded by the dwell-fatigue test in notched samples over the smooth bar is the ability to track fatigue damage near the crack since damage accumulation and crack initiation is largely localized to the notched section due to stress concentration at the notch while the damage elsewhere in the sample is relatively insignificant.

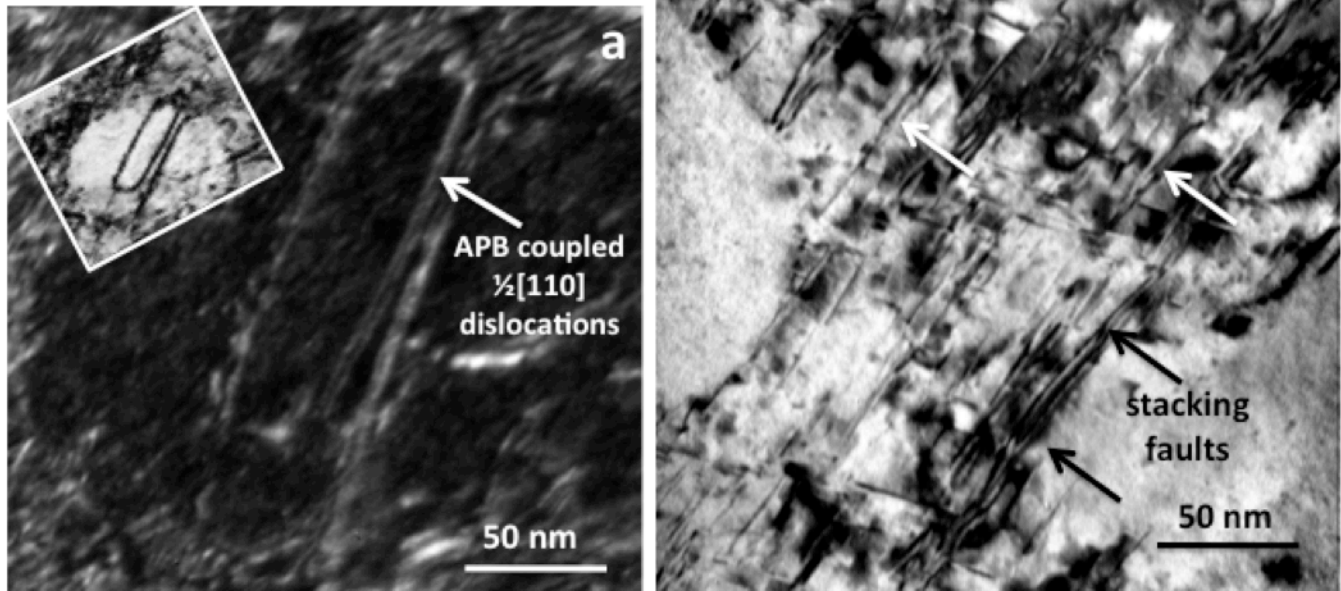


Figure 9. Bright field transmission electron images (TEM) showing (a) $\frac{1}{2}[110]$ superpartials within the γ' precipitate and (b) extensive intrinsic stacking faults in γ matrix channels in a grain from a region of high ΔK .

Fracture Morphology

The mostly intergranular nature of the fracture in the dwell-fatigued sample in this study is consistent with the previous reports [11] where the grain boundary failures have been reported in samples tested in air. The fracture morphology in time dependent and time independent fatigue fracture has been the subject of discussion for many years. Most consistent observation agreed upon many studies is the debit in fatigue life when the disk alloys are tested in air compared to vacuum. The shorter life seen in samples tested in air has been attributed to factors such as (i) oxygen diffusion to the slip band and (ii) grain boundary embrittlement due to oxygen promoting faster intergranular failure. Once again the fracture mode also depends on whether the cracks nucleate on the surface or subsurface. When the cracks nucleate on the surface the fracture remains intergranular right through the failure due to the oxygen embrittlement effect mentioned above. On the other hand, when the crack nucleates at the subsurface grains, the fracture mode reportedly remains transgranular until the crack reaches the surface, which then changes to an intergranular mode due to exposure to oxygen [11]. In our study the fracture morphology is uniform from the notched edge to the end of stable crack growth region, which is a mixture of intergranular and transgranular fracture. This suggests that the

cracks might have nucleated from multiple locations. The grains near the notch that have fractured in a transgranular fashion suggest that the crack nucleation or short crack growth occurred in those regions within the slip bands. On the other hand, the fractured carbide particles seen beneath the fracture surface could themselves be the crack nucleation sites ahead of the advancing crack.

Studies have shown that below 450°C fatigue occurs though time

independent damage mechanisms such a persistent slip band formation that promotes mostly transgranular failure. Above 550°C, especially under dwell cycles, contribution from creep damage mechanisms where thermally activated processes such as diffusion, cross slip, climb etc. become more prevalent.

Deformation

Planar slip band activity ahead of the advancing fatigue crack have been observed in a number of superalloys [3,14]. Boyd-Lee [10] has reported fracture morphology and slip band formation in RT fatigue study in Waspaloy as a function of ΔK . In that study, Boyd-Lee reported that crack nucleation occurred either within mode II slip bands or within carbide particles. During growth, at very low ΔK , only a few slip bands were observed while at very high ΔK numerous slip bands occupied in a cylindrical zone ahead of the crack tip covering many grains. It was also reported that variation in grain size in the alloy, allowed the transition zone from short crack to long crack growth regime to span over a wide range of ΔK . This clearly demonstrates the importance of ΔK , that allows for a large variation in the local stress conditions, which can have huge impact on the fatigue crack growth rate. This type of studies, although provide very useful information, are limited in scope since these observations are made on the surface of the samples and consequently can not accurately describe the

nature of crack tip interaction with local microstructural features such as γ and γ' precipitates and grain boundaries etc. which are critical to the fundamental understanding of deformation mechanisms during fatigue. However, detailed investigation of deformation substructures as a function of crack length from crack initiation to short crack growth to long crack growth is still lacking.

In γ/γ' based superalloys, the deformation modes can change substantially depending on the stress, temperature and loading conditions [7]. Typically at room temperature, irrespective of the loading conditions the main deformation mode is through the propagation of strongly coupled $\frac{1}{2}[110]$ dislocations, which do not leave any extended fault either in the gamma matrix or the precipitates. On the other hand, in addition to $\frac{1}{2}[110]$ dislocations, shearing through faulting and twinning has been observed at high temperatures especially under creep conditions. Extensive TEM analysis performed on the foils extracted from the dwell fatigue samples in this study also showed the presence of $\frac{1}{2}[110]$ dislocations, isolated faulting and extended faulting.

On the other hand, there were significant differences in subsidiary substructures between grains deformed under low and high K. First, the grain with the low K had significant density of intrinsic stacking faults in the gamma matrix compared to the high K grain which had significant activity of $\frac{1}{2}[110]$ unit dislocations. Secondly, within the gamma prime precipitates, the strongly coupled $\frac{1}{2}[110]$ dislocations were mostly co-planar, observed to lie mostly on (111) octahedral planes. On the other hand, significant cross-slip on to the cube planes was seen grains with higher ΔK .

These stacking faults seen in low K grain, arise from the dissociation of the $\frac{1}{2}[110]$ type unit dislocation, mainly driven by a low stacking fault energy, into two Shockley dislocations according to $\frac{1}{2}[110] - 1/6[112] + \text{ISF} + 1/6[211]$ in the gamma matrix. These Shockleys seen in these samples are indeed deformation-induced under dwell fatigue. Shockleys have been observed under creep deformation at intermediate temperatures and they are referred to as de-correlated dislocations. This essentially means that these individual Shockleys can now independently propagate despite the penalty introduced by the stacking fault at different velocities. Once dissociated, the mobility and therefore the shearing ability of these de-correlated Shockleys is now significantly depended on parameters such as, the resolved shear stress on individual shockleys and the Orowan stress, in other words, the stress required for these Shockleys to push through the γ channels in between the γ' precipitates.

Recent analytical and phase field modeling efforts by Unocic et al., [14] have shown that the resolved shear stress could be vastly different between the leading and the trailing Shockleys depending on the orientation of the grains with respect to the applied stress, the angle between the slip vector, or in other words the Burgers direction and the stress axis and the spacing between the precipitates. As a result, if the Orowan stress is high enough both the leading and the trailing partial will be able penetrate and accomplish the deformation without dragging any intrinsic fault. On the other hand, if the leading partial possess a higher resolved shear stress than the trailing partial, the mobility of these de-correlated dislocation will be severely affected that can lead to extensive faulting in the gamma matrix, because of the restriction placed by the spacing between the precipitates. This is presumably

may be the reason why extensive faulting in the gamma matrix occurs in the gamma matrix in a low K grain. This particular grain is presumably oriented such that the conditions were just right for faulting to occur for the reasons mentioned above where the resolved shear stresses were significantly different for the Shockleys along the slip direction. The resolved stress was probably insufficient even for the leading partial to be able to shear the γ' precipitate and as a result the stacking faults are mostly confined to the γ matrix. This is consistent with similar observations in a Ni-based superalloy, ME3, tested under creep conditions. The authors in that study, have reported extensive stacking fault in the gamma matrix and the bounding partials were seen locked in at the γ/γ' interfaces. Additional work is underway to determine the grain orientation with respect to the stress axis and the γ' precipitate size and distribution. On the other hand, the reason these short stacking faults in the gamma matrix are not prevalent in a high K grain may possibly be due to higher and sufficient resolved stress levels favoring $\frac{1}{2}[110]$ dislocations.

With respect to the substructures seen within the γ' precipitate, cube cross-slip has been known to occur for a long time under tensile loading at high temperatures in single crystals of binary and alloyed Ni_3Al , especially in the anomalous yield strength regions. The cube cross slip has been reported to occur over a wide temperature regime due to the lower APB energy on the {100} cube planes compared to {111} octahedral planes. Primary cube slip has been observed in Alloy MERL 76 during high temperature high cycle fatigue condition [8]. However, this has been the first time such cube slip has been observed in γ' precipitates in a γ/γ' multi-component superalloy under dwell-fatigue condition. However, it is unclear at this point why cube slip is more prevalent in grains with low Δk compared to high K grain where the slip is mostly seen coplanar. It is speculated that the severe local stress conditions imposed by higher K, somehow prevent the dissociation of $\frac{1}{2}[110]$ unit dislocations.

Additional TEM foils are currently being extracted from and below the fracture surface for further analysis of the deformation mechanism.

Conclusions

The fracture morphology indicates that the fracture during dwell-fatigue in samples tested in air reveals a mixture is intergranular and transgranular failure.

The microstructure below the fracture surface indicated that the crack frequently nucleates in grain triple points, especially where the twins within the grain intersects the grain boundaries.

Sample that was exposed to air during the test provided regions below the fracture surface with recrystallized grains with a significant loss of γ' precipitates.

TEM analysis indicates that deformation substructures vastly differ in grains with varying K. The difference in the nature of substructures is attributed to the grain orientations and the local stress intensity factors.

References

1. N.J. Hide, M.B. Henderson, P.A.S. Reed, "Effects of grain and

- precipitate size variation on creep-fatigue behavior of Udimet 720Li in both air and Vacuum”, *Superalloys 2000*, TMS; (2000) 495-503.
2. G. Onofrio, G.A. Osinkolu and M. Marchionni, “Fatigue crack growth of Udimet 720Li superalloy at elevated temperature, *Int. J. Fatigue*, 23, (2001) 87-895.
 3. Andre Pineau and S.D. Antolovich, “High Temperature fatigue of Nickel-base superalloys – A review”, *Engg. Failure Anal.*, 16 (2009) 2668-2697.
 4. P.A.S. Reed and I. Sinclair, “Temperature and environment effects on mode I crack propagation in Ni-base superalloys”, Final report on MOD research contract 2040/515/MA, University of Southampton.
 5. W.W. Milligan and S.D. Antolovich, “Yielding and deformation behavior of single crystal superalloy PWA 1480”, *Met. Trans.* 18A (1987) 85-95.
 6. G.B. Viswanathan, P.M. Sarosi, M.F. Henry, D.D. Whitis, W.W. Milligan, M.J. Mills, “Investigation of creep deformation mechanisms at intermediate temperatures in René 88 DT” *Acta Materialia*, 53,10,(2005), 3041-3057.
 7. G. B. Viswanathan, S. Karthikeyan, P. M. Sarosi, R. R. Unocic and M. J. Mills: “Microtwinning during intermediate temperature creep of polycrystalline Ni-based superalloys: mechanisms and modeling”, *Philosophical Magazine A*, 86, 29-31, 2006, 4823-4840.
 8. R.V. Miner, J. Gayda and R.D. Maier, “Fatigue and Creep – Fatigue deformation of several Ni-base superalloys at 650C, *Metallurgical Transaction A*, 13A, (1982) 1755-1765.
 9. E.J. Payton, P.J. Phillips, M.J. Mills, Semi-automated characterization of the γ' phase in Ni-based superalloys via high resolution backscatter imaging. *Materials Science and Engineering A 527* (2010) 2684–2692.
 10. Boyd-Lee, “Fatigue crack growth resistant microstructures in polycrystalline Ni-base superalloys for aeroengine”, *Intl. Journal of Fatigue*, 21, (1999) 393-405.
 11. M. J. Caton and S.K. Jha, “Small fatigue crack growth and failure mode transitions in a Ni-base superalloy at elevated temperature”, *Intl. Journal of Fatigue*, 32, (2010) 1461-1472.
 12. J.Miao, T.M. Pollock, J. W. Jones, “Crystallographic fatigue crack initiation in Ni-base superalloy Rene 88DT at elevated temperature”, *Acta Materialia* 57 (2009) 5964-5974.
 13. J. Telesman, T.P. Gabb, A. Garg, P. Bonacuse and J. Gayda, “Effect of microstructure on the time dependent fatigue crack growth behavior in a P/M turbine disk alloy”, *Superalloys 2008*
 14. Patrick J. Phillips, Raymond R. Unocic, L. Kovarik, David Mourer, Dan Wei and Michael J. Mills, *Scripta Materialia*, 62, 10 (2010), 790-793.
 15. M. J. Caton, S. K. Jha, A. H. Rosenberger, and J. M. Larsen divergence of mechanisms and the effect on the Fatigue life variability of Rene` 88 DT” *Superalloy 2008*
 15. Caton MJ, Jha SK, Rosenberger AH, Larsen JM. Divergence of mechanisms and the effect on the fatigue life variability of Rene`88DT. *Superalloys 2004*, eds. Green KA, Pollock TM, Harada H, Howson TE, Reed RC, Schirra JJ, Wanston, The Minerals, Metals and Materials Society, Warrendale, PA, 2004, 305-312.
 16. R.R. Unocic, N. Zhou, L. Kovarik, C. Shen, Y. Wang, M.J. Mills, “Dislocation decorrelation and relationship to deformation microtwins during creep of a γ' precipitate strengthened Ni-based superalloy”, *Acta Materialia* 59 (2011) 7325–7339.
 17. P. Veysiere, *Phil. Mag. A* 50 (1984) 189–203.
 18. P. Caron, T. Khan, *Phil. Mag. A* 60 (1989) 267–281.
 19. Yu Jinjiang *, Sun Xiaofeng, Jin Tao, Zhao Nairen, Guan Hengrong, Hu Zhuangqi High temperature creep and low cycle fatigue of a nickel-base superalloy, *Materials Science and Engineering A 527* (2010) 2379–2389.